Int. J. Heat Mass Transfer. Vol. 25, No. 8, pp. 1113–1126, 1982
Printed in Great Britain

0017-9310/82/081113-14 $03.00/0
Pergamon Press Ltd.

HEAT AND MASS TRANSFER IN TWO-PHASE FLOW— A MATHEMATICAL MODEL FOR LAMINAR FILM FLOW AND ITS EXPERIMENTAL VALIDATION

J. R. CONDER, D. J. GUNN and M. ASHFAQ SHAIKH
Department of Chemical Engineering, University College of Swansea, Singleton Park, Swansea, West Glamorgan, SA2 8PP, U.K.

(*Received* 21 *July* 1981 *and in final form* 13 *January* 1982)

Abstract—A mathematical model is presented for the vaporisation of liquid from a laminar film flowing down the inside surface of a smooth tube into a countercurrent laminar flow of gas. The partial differential equations that describe temperature and composition distributions are integrated across the tube to give a set of four coupled ordinary differential equations. A numerical method for the solution of the equations is proposed and examined; the method is posed to solve the transient response for heat and mass transfer. A satisfactory solution is found for a range of space and time intervals. The mathematical model has been validated by experimental measurements on a falling film evaporator with evaporation occurring at sub-boiling temperatures from a laminar liquid film into a laminar gas stream. The performance of the evaporator is assessed.

NOMENCLATURE

A, $(1 - u_g \Delta t/\Delta z)$;
B, $u_g \Delta t/\Delta z$;
C_i, $P_{j,i}(1 - \alpha\Delta t) + P^*_{j,i}\alpha\Delta t$;
C, heat capacity (of liquid if unsubscripted);
d, tube diameter;
D, $(1 - u_z\Delta t/\Delta z)$;
D_m, molecular diffusivity;
E, $u_z\Delta L/\Delta z$;
f, function defined by equation (19);
F, function defined by equation (15);
F_j, $S_{j,i}(1 - \beta\Delta t) + \beta\Delta t T_w - \varepsilon\Delta t(I_{j,i} - T_{j,i}) - \eta(P^*_{j,i} - P_{j,i})\Delta t$;
g, acceleration due to gravity;
G, $(1 - u_g\Delta t/\Delta z)$;
h, heat transfer coefficient;
h_m, mass transfer coefficient;
H, $u_g\Delta t/\Delta z$;
$I_{j,i}$, interface temperature;
k, thermal conductivity;
K_j, $T_{j,i}(1 - \gamma\Delta t - \theta\Delta t) + \gamma\Delta t T_w + \theta I_{j,i}\Delta t$;
L, tube length;
n_1, $\pi k_g L/(4W_g C_g)$;
n_2, $D_m L/(u_g d^2)$;
N, mass flux;
Nu, Nusselt number, hd/k;
$p, P_{j,i}$, gas phase partial pressure of diffusing component;
$P^*, P^*_{j,i}$, partial pressure of diffusing component at gas–liquid interface;
Pr, Prandtl group, $C\mu/k$;
r, radial co-ordinate;
R, radius of tube;
R_G, gas constant;
Re, Reynolds number, $du\rho/\mu$;
$S_{j,i}$, liquid temperature;
Sc, Schmidt group, $\mu/\rho D_m$;
Sh, Sherwood group $h_m d/D_m$;
t, time;
$T, T_{j,i}$, temperature, gas phase temperature;
T_a, absolute temperature;
u, velocity;
W, mass rate of fluid flow in tube;
y, transverse co-ordinate;
Z, axial co-ordinate, measured from bottom of tube.

Greek symbols

α, $4\psi h_m/d$;
β, $h_z/(\delta\rho C)$;
γ, $4h_g(1 - \psi)/(d\rho_g C_g)$;
Γ, volumetric flow rate of liquid down unit periphery of tube,
δ, film thickness;
Δ, difference;
ε, $h_g/(\delta\rho C)$;
η, $h_m\lambda/(\delta\rho C R_G T_a)$;
θ, $4\psi g_g/(d\rho_g C_g)$;
λ, latent heat of vaporisation;
μ, viscosity;
ρ, density;
ϕ, flux of heat;
ψ, wetted fraction of tube perimeter.

Subscripts

a, absolute temperature;
g, gas or gas at outlet;
i, inlet;
ℓ, liquid;
m, mass;
s, surface;
w, wall.

INTRODUCTION

DURING the past several years heat transfer to single component mixtures of liquid and vapour rising in tubes in two-phase flow has been an important research study mainly because of applications to boiling systems, including thermonuclear systems. An account of much of this work has been given by Collier [1].

The vaporisation of a liquid into an inert gas stream has not received as much attention, even though there are applications of heat transfer where the presence of an inert gas, for example, may be a very important factor in determining heat transfer rates. Thus distillation of a volatile component from a mixture with involatiles by treating the mixture with a flow of heated inert gas may be a very suitable method of separation particularly when the volatile component is heat-sensitive. Another application where there may be problems with heat-sensitive materials is found in production gas chromatography. In this method of separation, components to be separated are mixed with, or vaporised into, an inert carrier gas before passing into the separation column. Heat-sensitive liquids may be vaporised into the gas streams at temperatures that are low enough to avoid significant thermal degradation [2].

In the falling-film vaporiser, liquid to be vaporised flows down the inside of a vertical cylindrical tube in the same direction as, or in the opposite direction to, the stream of inert gas. Heat is transferred to the vaporising liquid by, for example, condensing steam on the outside of the tube.

A mathematical model for heat and mass transfer from a falling film to a stream of inert gas in countercurrent flow is formulated. The expression of the mathematical model in a form suitable for numerical solution is described, and the operating characteristics of the numerical method are discussed.

The model is formulated for gas and liquid in countercurrent flow. In cocurrent flow a simpler method or the same method may be used.

THEORY

At steady state heat is transferred from the heated wall to liquid flowing down the inside surface of a vertical tube as shown in Fig. 1. Liquid is evaporated at the liquid surface into the gas phase, and there is heat exchange between gas and liquid. When flow is laminar in both phases equations for the conservation of momentum for each phase include the known physical properties of density and viscosity, while the equations for conservation of heat and mass include known densities and heat capacities in addition. The set of partial differential equations includes derivatives with respect to the axial coordinate and the tube radial coordinate. The equations are defined by a set of boundary conditions and in countercurrent flow the inlet conditions for gas and liquid are defined at the opposite ends of the tube.

The non-linearity of the equations arises mainly from the strongly non-linear dependence of vapour pressure upon temperature. Thus at the gas–liquid interface vaporisation takes place at the temperature of the interface, so that the vapour pressure is equal to the saturation pressure at the interface temperature. The non-linearity combined with the boundary-value nature of the process equations thus poses a major problem in demands of computational time and store. However, a significant reduction in computational scale arises from a physical analysis based upon the small thickness of the film.

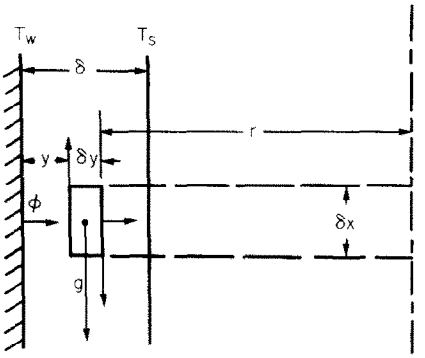

FIG. 1. Diagram of evaporator.

Heat transmission through the liquid film

Consider a thin film of liquid in laminar motion flowing down the smooth inside surface of a round, vertical tube. Gas also in laminar motion flows countercurrent to the liquid, and the tube wall is held at a constant temperature above the entrance temperatures of both gas and liquid.

Liquid motion is taken to be free from wave motion and other disturbances at the inlet, the thickness of the film is small compared to the tube radius, and interfacial shear due to gas motion is sufficiently small to be neglected. The mass flow of liquid flowing down unit periphery of the tube is to be found on integration of the velocity distribution. It is

$$\Gamma = \frac{\rho^2 g \delta^3}{3\mu}. \tag{1}$$

As the film is thin, axial conduction may be neglected in comparison with transverse conduction through the film. The differential equation for conservation of thermal energy in the fluid element of Fig. 1 is

$$k\frac{\partial^2 T}{\partial y^2} = u\rho C\frac{\partial T}{\partial z}. \tag{2}$$

This equation may be integrated with the aid of the observation that $\partial T/\partial z$ does not vary significantly over the thin film except over a very short entrance section at the top of the column to give

$$k\left[\left(\frac{\partial T}{\partial y}\right)_\delta - \left(\frac{\partial T}{\partial y}\right)_w\right] = \Gamma C\left(\frac{\partial T_g}{\partial z}\right) \tag{3}$$

where $(\partial T_g/\partial z)$ is the average value of the axial temperature gradient for the film.

It is convenient to introduce ϕ_w as the heat flux at the wall of the tube. Since the liquid phase is thin and T_ℓ is its mean mixed temperature, the gradient at the wall $(\partial T/\partial y)_w$ is closely approximated by $2(T_w - T_\ell/\delta$, so that to the same degree of approximation, using equation (1),

$$\phi_w = \frac{2k(T_w - T_\ell)}{\delta} = \left(\frac{8k^3\rho^2 g}{3\mu\Gamma}\right)^{1/3}(T_w - T_\ell)$$

or

$$\phi_w = h(T_w - T_\ell) \tag{4}$$

where the heat transfer coefficient h is given by

$$h = \left(\frac{8k^3\rho^2 g}{3\mu\Gamma}\right)^{1/3}. \tag{5}$$

Heat transfer to the gas phase

For gas in laminar motion in a round tube with axially symmetric boundary conditions, the partial differential equation describing the transport of heat is

$$k_g\left(\frac{1}{r}\frac{\partial}{\partial r}r\frac{\partial T}{\partial r}\right) + k_g\frac{\partial^2 T}{\partial z^2} - 2u_g\left(1 - \frac{r^2}{R^2}\right)\rho_g C_g\frac{\partial T}{\partial z} = 0 \tag{6}$$

where ρ_g is the density and C_g is the specific heat of the gas, and

$$2u_g\left(1 - \frac{r^2}{R^2}\right)$$

is the velocity profile. The boundary conditions are

$$T_g = T_s \text{ at } r = R - \delta, \text{ the interface} \tag{7}$$

and

$$\frac{\partial T_g}{\partial r} = 0 \text{ at } r = 0.$$

Graetz [3] neglected $\partial^2 T/\partial z^2$ in equation (6) and solved the equation for the condition of fixed temperature at the surface of a cylindrical tube. His solution gave the "mixing cup" temperature in the form of an infinite series when the surface temperature was zero for $z < 0$, and T_s for $z > 0$

$$\frac{T_g - T_{gi}}{T_s - T_{gi}} = 1 - 8F(n_1) \tag{8}$$

where T_{gi}, T_g and T_s are the inlet, outlet and surface temperatures respectively and $F(n_1)$ is the convergent infinite series

$$F(n_1) = 0.10238\,e^{-14.627n_1} + 0.0122\,e^{-89.22n_1} + 0.00237\,e^{-212n_1}\ldots \tag{9}$$

Here n_1 is the dimensionless group $\pi k_g L/4W_g C_g$, where W_g is the mass flow rate of gas in the tube, and L is the tube length.

It is convenient in the present work to use a heat transfer coefficient for the whole tube based upon an average temperature difference. The use of a logarithmic mean temperature difference is not correct in the usual form because of the variation of the heat transfer coefficient with z. The logarithmic mean temperature difference is also very sensitive to the fluid temperature when close to the surface temperature. The heat transfer coefficient based upon the arithmetic average of the inlet and outlet temperature differences does not show this undesirable sensitivity. In terms of the Graetz solution the coefficient has the form [4]

$$\frac{h_g d}{k_g} = \frac{2W_g C_g}{\pi k_g L}\frac{1 - 8F(n_1)}{1 + 8F(n_1)}. \tag{10}$$

Mass transfer to the gas phase

The analogous relationships between heat and mass transfer may be expressed [5] in the form

$$Nu = f(Re \cdot Pr)$$

$$Sh = f(Re \cdot Sc)$$

so that if the relationship between the Nusselt, Reynolds and Prandtl groups is given by equation (10), the analogous relationship for mass transfer is

$$\frac{h_m d}{D_m} = \frac{2\pi d^2 u_g}{4\pi D_m L}\frac{1 - 8F(n_2)}{1 + 8F(n_2)} \tag{11}$$

where $F(n_2)$ is the infinite series of equation (9) and n_2 is the dimensionless group

$$\pi D_m L \Big/ \left(4\frac{\pi d^2}{4}u_g\right).$$

In terms of dimensionless groups equation (11) may be expressed

$$Sh = \frac{1}{2}Re\,Sc\,(d/L)\left(\frac{1 - 8F(n_2)}{1 + 8F(n_2)}\right). \tag{12}$$

The equations of conservation for heat and mass

By integrating over the transverse dimension, and establishing transfer coefficients, the dimensionality of the differential equations has been reduced so that the equations of conservation at steady state may be expressed as three simultaneous ordinary differential equations. However, in countercurrent flow the inlet conditions of gas and liquid are given at opposite ends of the tube, and as such boundary conditions give rise to difficulty in computation when the equations are not linear, the equations of conservation are expressed in transient form. The transient equations still retain the same boundary conditions, but start from initial conditions that are fixed for both gas and liquid over the whole length of the tube.

The equations are given in reduced form below:

Conservation of heat for the liquid phase

$$h(T_w - T_\ell) - \Gamma\rho C\frac{\partial T_\ell}{\partial z} - h_g(T_s - T_g) - \frac{\lambda}{R_G T_a}(p_s - p_g) = \delta\rho C\frac{\partial T_\ell}{\partial t}. \tag{13}$$

The first term represents heat transfer from the wall to the liquid, the second is the change in heat content of the liquid due to the axial temperature gradient, the third is heat transferred from liquid to gas and in the fourth term λ is the latent heat of vaporisation so that this term represents the thermal requirement for vaporisation. The sum of the thermal energy terms then gives the change of liquid-phase enthalpy with time as shown on the RHS of equation (13). ψ is defined as the ratio of wetted to total tube periphery and is introduced to allow for partial wetting of the tube.

Conservation of heat for the gas phase

$$h_g(T_w - T_g)(1 - \psi) + h_g(T_s - T_g)\psi - u_g\rho_g C_g \frac{d}{4}\frac{\partial T_g}{\partial z} = \frac{d}{4}\rho_g C_g \frac{\partial T_g}{\partial t}. \quad (14)$$

The first term represents heat transferred directly from the unwetted wall to the gas, the second represents heat transferred from liquid phase to the gas, the third term is the enthalpy change due to the axial temperature gradient and the RHS is the change of gas-phase enthalpy with time.

Conservation of mass for the gas phase

$$h_m(p_s - p)\psi - u_g \frac{d}{4}\frac{\partial p_g}{\partial z} = \frac{d}{4}\frac{\partial p_g}{\partial t}. \quad (15)$$

As the rate of vaporisation in the experiments was much less than the liquid flowrate a separate conservation equation for the liquid phase was not necessary.

The initial conditions define the liquid and gas phase temperatures along the length of the tube at $t = 0$, viz. $T_l = T_{li}$, $T_g = T_{gi}$, $p = 0$. The boundary conditions are

$$T_g = T_{gi} \quad \text{at } z = 0,$$
$$T_l = T_{li} \quad \text{at } z = L, \quad (16)$$

and $$p = 0 \quad \text{at } z = 0.$$

One further necessary condition is to define p_s in equation (15). The pressure p_s is the partial pressure of liquid at the interface, that is to say the saturation pressure of liquid at the interface temperature T_s. The interface temperature is not explicit in the equations, but may be found from the wall and liquid temperatures during the course of the computation.

THE NUMERICAL METHOD

In the numerical method first order derivatives are replaced by suitable finite difference forms. The derivatives may be represented by forward, backward or central differences approximations, and in addition, space derivatives may be defined at known or unknown points in time. To avoid stringent restrictions on the length of the time step it was decided to use an implicit method. The column was divided into axial segments of the length Δz. If the subscript j denotes position and the subscript i denotes time, the derivatives in equations (13)–(15) may be expressed by the following finite difference approximations:

$$\frac{dT_g}{dz} = \frac{T_{j+1,i+1} - T_{j,i+1}}{\Delta z}$$

where T is the gas temperature,

$$\frac{dT_l}{dz} = \frac{S_{j,i+1} - S_{j-1,i+1}}{\Delta z}$$

where S is the liquid temperature,

$$\frac{dp}{dz} = \frac{P_{j+1,i+1} - P_{j,i+1}}{\Delta z} \quad (17)$$

where P is the partial pressure in the gas phase,

$$\frac{dT_g}{dt} = \frac{T_{j,i+1} - T_{j,i}}{\Delta t},$$

$$\frac{dT_l}{dt} = \frac{S_{j,i+1} - S_{j,i}}{\Delta t},$$

$$\frac{dp}{dt} = \frac{P_{j,i+1} - P_{j,i}}{\Delta t}.$$

If the approximations are now substituted into equations (13)–(15), three sets of finite difference equations are obtained, one set corresponding to each equation. Terms other than those corresponding to equations (17) are defined at the known time level i.

Thus on setting $A = 1 - u_g\Delta t/\Delta z$, $B = u_g\Delta t/\Delta z$, and $C_j = P_{j,i}(1 - \alpha\Delta t) + P^*_{j,i}\alpha\Delta t$, where $P^*_{j,i}$ is the saturation vapour pressure at the jth node and ith time level and $\alpha = 4\psi h_m/d$, the following matrix equation is obtained from equation (15):

$$\begin{bmatrix} B & 0 & 0 & 0 & \cdots & 0 \\ A & B & 0 & 0 & \cdots & 0 \\ 0 & A & B & 0 & \cdots & 0 \\ \cdot & \cdot & \cdot & \cdots & \cdots & \cdot \\ 0 & 0 & 0 & \cdots & A & B \end{bmatrix} \begin{bmatrix} P_{2,i+1} \\ P_{3,i+1} \\ \vdots \\ \vdots \\ P_{n,i+1} \end{bmatrix} = \begin{bmatrix} C_1 - AP_{1,i+1} \\ C_2 \\ \vdots \\ \vdots \\ C_n \end{bmatrix} \quad (18)$$

The matrix of coefficients is lower bidiagonal, and the equation may be solved by successive substitution starting from the first row. $P_{1,i+1}$, the partial pressure of the vaporising component in the gas phase at its inlet, is a boundary condition.

If $D = 1 - u_l\Delta t/\Delta z$, $E = u_l\Delta t/\Delta z$ and $F_j = S_{j,i}(1 - \beta\Delta t) + \beta\Delta t T_w - \varepsilon\Delta t(I_{j,i} - T_{j,i}) - \eta(P^*_{j,i} - P_{j,i})\Delta t$ where the liquid phase velocity $u_l = \Gamma/(\pi d\delta)$, $\beta = h_l/(\delta\rho C)$, $\varepsilon = h_g/(\delta\rho C)$, $\eta = h_m\lambda/(\delta\rho C R_G T_s)$, and $I_{j,i}$ is the interface temperature, equation (25) after finite difference substitution takes the upper bidiagonal matrix form

$$\begin{bmatrix} E & D & 0 & 0 & \cdots & 0 \\ 0 & E & D & 0 & \cdots & 0 \\ 0 & 0 & E & D & \cdots & 0 \\ \cdot & \cdot & \cdot & \cdot & \cdots & \cdot \\ 0 & 0 & 0 & \cdots & \cdots & E \end{bmatrix} \begin{bmatrix} S_{1,i+1} \\ S_{2,i+1} \\ \vdots \\ \vdots \\ S_{n-1,i+1} \end{bmatrix} = \begin{bmatrix} F_2 \\ F_3 \\ \vdots \\ \vdots \\ F_n - DS_{n,i+1} \end{bmatrix} \tag{19}$$

Since the matrix of coefficients is upper bidiagonal, the equation may be solved by back substitution, starting from the last row. $S_{n,i+1}$, the temperature of the liquid phase at its inlet, is a boundary condition.

The third matrix equation may be obtained from equation (22) by setting $G = 1 - u_g\Delta t/\Delta z$, $H = u_g\Delta t/\Delta z$ and $K_j = T_{j,i}(1 - \gamma\Delta t - \theta\Delta t) + \gamma\Delta t T_w + \theta I_{j,i}\Delta t$, where $\gamma = 4h_g(1 - \psi)/(d\rho_g C_g)$ and $\theta = 4\psi h_g/d\rho_g C_g)$. It is

$$\begin{bmatrix} H & 0 & 0 & \cdots & 0 \\ G & H & 0 & \cdots & 0 \\ 0 & G & H & \cdots & 0 \\ \cdot & \cdot & \cdot & \cdots & \cdot \\ 0 & 0 & 0 & G & H \end{bmatrix} \begin{bmatrix} T_{2,i+1} \\ T_{3,i+1} \\ \vdots \\ \vdots \\ T_{n,i+1} \end{bmatrix} = \begin{bmatrix} K_1 - GT_{1,i+1} \\ K_2 \\ \vdots \\ \vdots \\ K_{n-1} \end{bmatrix} \tag{20}$$

The matrix of coefficients is lower bidiagonal in form, so that the equation may be solved by forward substitution starting from the first row. $T_{1,i+1}$, the temperature of the gas at inlet, is a boundary condition.

The numerical method is implicit. However the relationship between the saturated vapour pressure and temperature at the interface is so highly non-linear, that an extended implicit scheme would require nested iterations at each time step. The alternative explicit method would be subject to the well-known constraints on time and length intervals, but more severe because of the nature of the non-linearity. The method described above is free from the requirement of iteration because the non-linearity is defined at the known time level, while the matrix equations may be solved by efficient recursion formulas because of the bidiagonal forms of the coefficient matrices.

Estimation of the interface temperature

An estimate of the interface temperature is required to advance the computation to the next time step, so that it was particularly necessary to generate an accurate estimate of this important variable at each time step.

At the top of the tube, the point of liquid entry, it was expected that the interface temperature would be close to the liquid temperature, while in the major part of the tube the temperature distribution should be closely linear, so that the wall temperature and the average liquid temperature are sufficient to determine the interface temperature. Temperature distributions at liquid inlet and in the major part of the tube are illustrated in Fig. 2. The interface temperature is

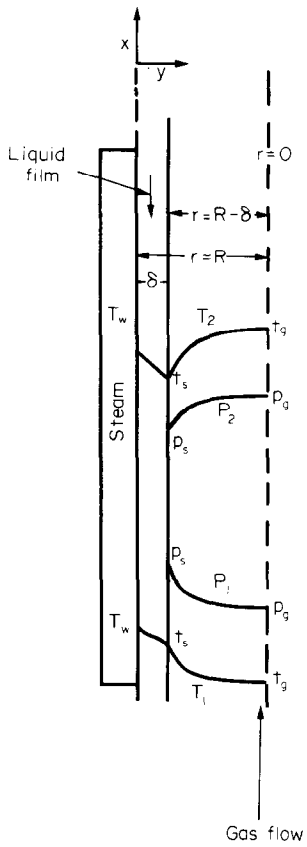

FIG. 2. Illustration of temperature and pressure distributions in evaporator. T_1, P_1: profiles in major part of tube, T_2, P_2: profiles at liquid inlet.

defined in terms of the wall and liquid temperature in the linear region by the equation

$$T_s = 2T_l - T_w. \tag{21}$$

Two consistent expressions were used for the estimation of interface temperatures during the computations. Equation (22) employed weighting factors

$$T_s = T_l e^{-8(L-z)/L} + (2T_l - T_w)(1 - e^{-8(L-z)/L}) \tag{22}$$

The weighting factors $e^{-8(L-z)/L}$ and $(1 - e^{-8(L-z)/L})$ ensured that the interface temperature was similar to the liquid temperature at the top of the tube where z was close to L, while in the major part of the tube the interface temperature was given by equation (21).

The second method of estimation was less time consuming and as the calculated distributions of temperature and pressure were almost identical for both methods, the second method was adopted. In the second method starting from the base of the tube, $2T_l - T_w$ was compared with T_g; if $2T_l - T_w > T_g$, T_s was set to $2T_l - T_w$. When $2T_l - T_w < T_g$, but $T_g < T_l$, T_s was set to the same value as that just calculated in the segment below, while if $2T_l - T_w < T_g$ and $T_g > T_l$, the interface temperature was set to T_l. This method gave satisfactory and consistent estimates of interface temperature for all hot and cold liquid entries and combinations of flow rates and gas inlet temperatures.

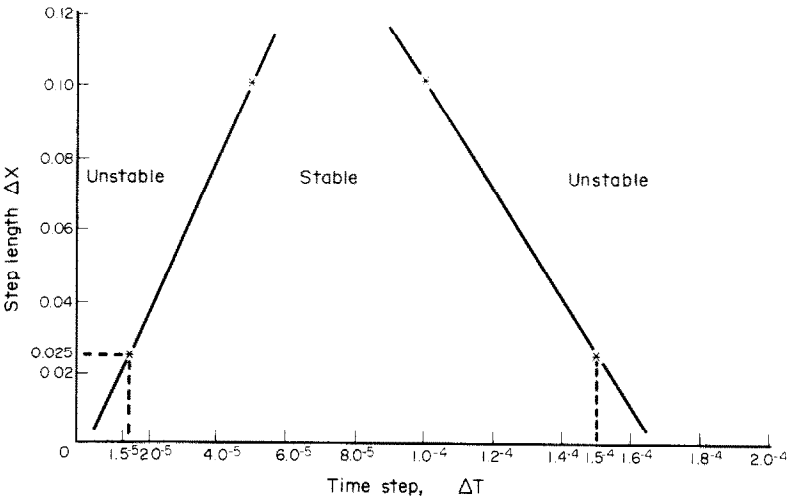

FIG. 3. Stability boundaries for numerical computation.

Characteristics of the numerical solution

A series of numerical experiments was carried out to examine the range of validity of the numerical solution. For a given increment of tube length Δz, the time interval was varied and the solution integrated from a given set of initial conditions forward in time until the temperature and partial pressure distributions became steady. For some combinations of time and distance intervals, the temperature and pressure distribution did not converge to the independent conditions, but oscillated and showed unstable behaviour. The range of stable and unstable behaviour is illustrated in Fig. 3; it may be seen that when Δz is small a stable solution may be obtained for a wide range of Δt. Stable solutions may also be obtained when Δz is significantly larger, but the range of Δt for stability is much smaller.

EXPERIMENTAL VERIFICATION OF THE MODEL

The mathematical model for heat transfer in laminar film flow is a model without disposable parameters when the tube is fully wetted. As a fully-wetted tube is desirable to vaporise liquid, the experimental programme of heat transfer measurements was carried out for a range of two-phase flows at liquid rates that were sufficiently high to completely wet the tube surface. Heat transfer was measured for both single-phase flow and two-phase countercurrent flow of gas and liquid.

Experimental arrangement

A detailed drawing of the falling film evaporator is shown in Fig. 4. The evaporator tube was constructed from copper, 5 ft 10 in. long, 1/2 in. I.D. and 19/32 in. O.D. The upper end of the tube was bevelled to a sharp edge and carefully honed so that liquid distribution was uniform around the periphery of the tube. The tube was carefully adjusted to give good vertical alignment and the lower end was serrated so that liquid distribution could be observed from the points of the serrations. Liquid entered the glass T at the top of the evaporator by means of 1/4 in. copper pipe in the bottom flange; a thermocouple was placed just below the top of the tube to measure liquid inlet temperature. A second thermocouple was placed on the axis of the evaporator tube at the top of the heated section to measure the gas exit temperature. At the base of the evaporator liquid overflowed and gas entered through 1/2 in. copper lines. A thermocouple was placed in this section to measure the entry temperature of the gas.

A flow diagram of the apparatus is shown in Fig. 5. The carrier gas, nitrogen, was metered and passed through a preheater consisting of 19 ft of 1/2 in. stainless steel pipe wrapped with nichrome wire and insulation. The current in the nichrome wire was controlled by a variac to give the desired gas temperature before entering the evaporator.

On leaving the evaporator, vapour was stripped from the gas by a water-cooled condenser followed by absorption columns containing polyethylene glycol supported on packing. Clean carrier gas was compressed and recycled. The absorption columns could be by-passed during start-up, or when no liquid feed was introduced.

Geraniol liquid feed was metered by a calibrated gear pump, and heated by an electrical preheater that contained 5 ft of 1/4 in. dia copper tube. The temperature of the liquid leaving the base of the evaporator was reduced by heat exchange before recycling to minimise losses due to vaporisation.

Steam from the laboratory supply passed through a condensate separator connected to a float trap, and through a strainer before pressure reduction. The low pressure side of the reducer was connected to a second float trap to ensure that only dry steam entered the jacket.

The iron–constantan thermocouples used were calibrated against NPL certificated thermometers.

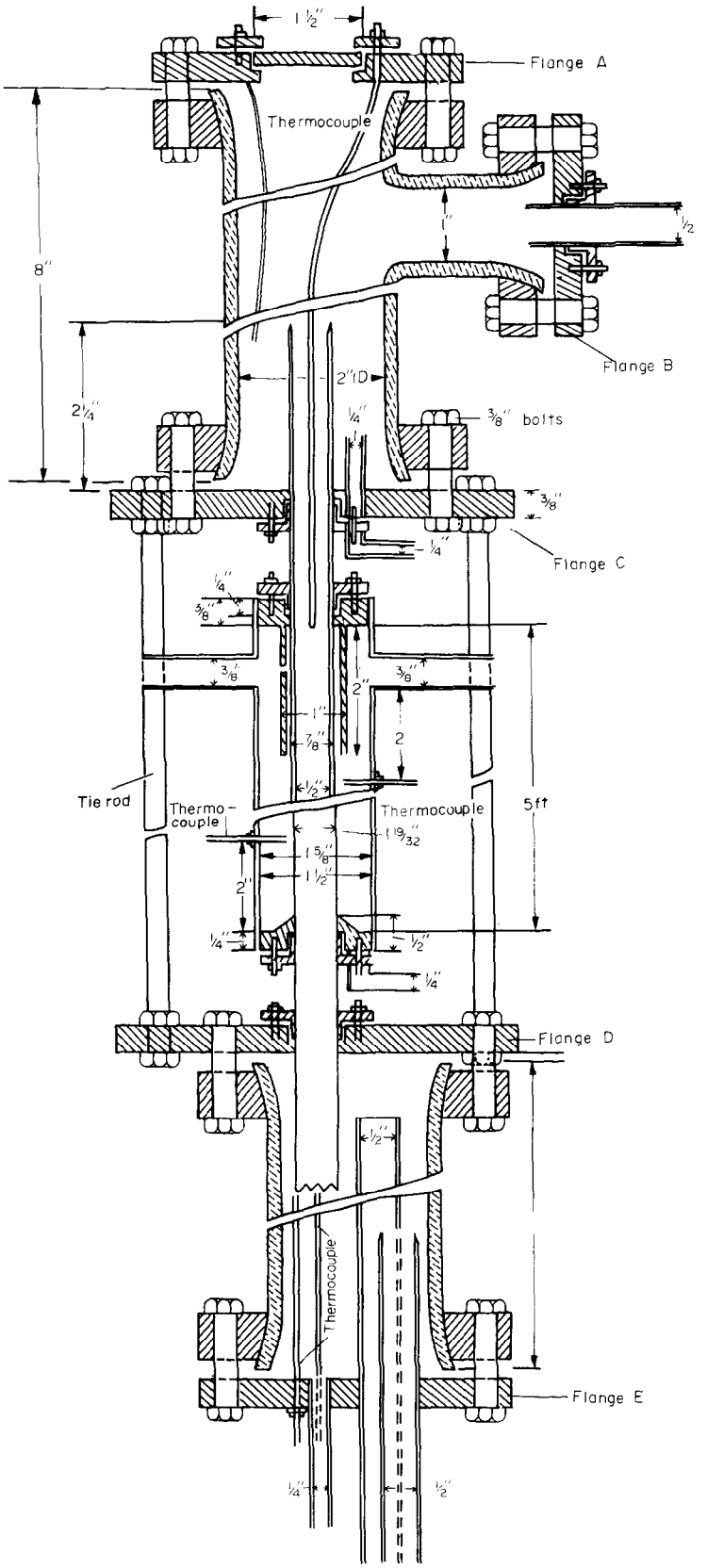

FIG. 4. Construction of falling film evaporator.

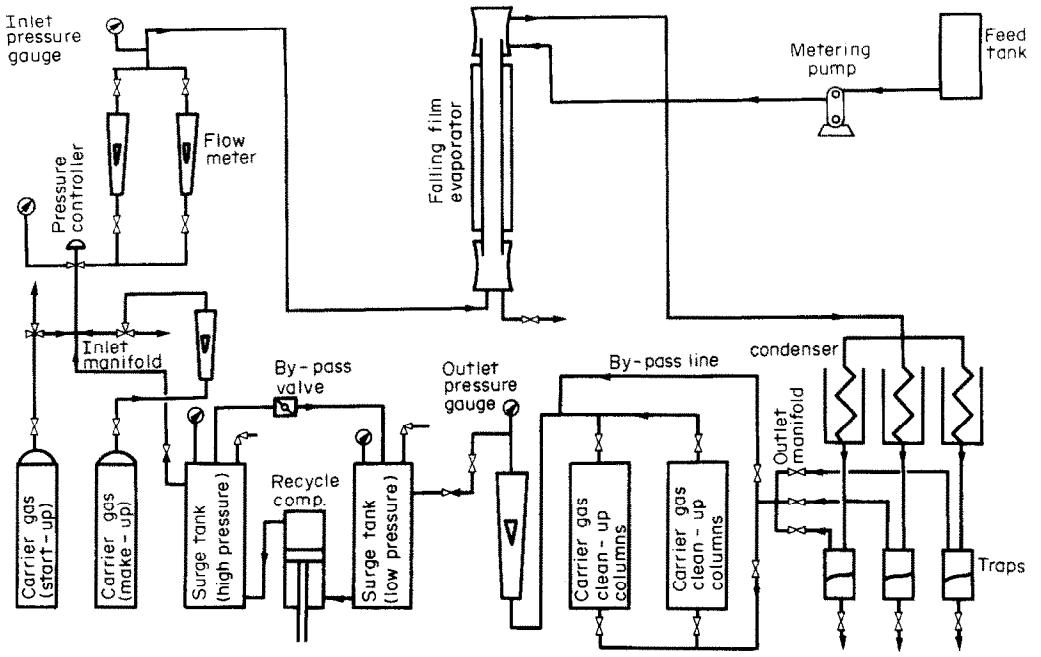

FIG. 5. Flow scheme of apparatus.

Experimental procedure

The system was started up and left running overnight to attain steady state.

The condensate was collected when the gas alone passed through the evaporator and measured at intervals of 5–10 min. The gas inlet and outlet temperatures were recorded on a strip chart.

The liquid preheater and feed pump were then switched on and set to predetermined conditions. The overflow valve connected to the bottom chamber was set to monitor a constant liquid level in the bottom chamber so as to maintain a liquid seal, and prevent flooding of the evaporator tube.

The liquid temperature was monitored continuously and when constant for 15–20 min, gas and liquid temperature were noted and several condensate measurements were made. At the end of a run the liquid feed pump was switched off.

After 8 h operation the absorption columns were interchanged and the used one was purged by passing

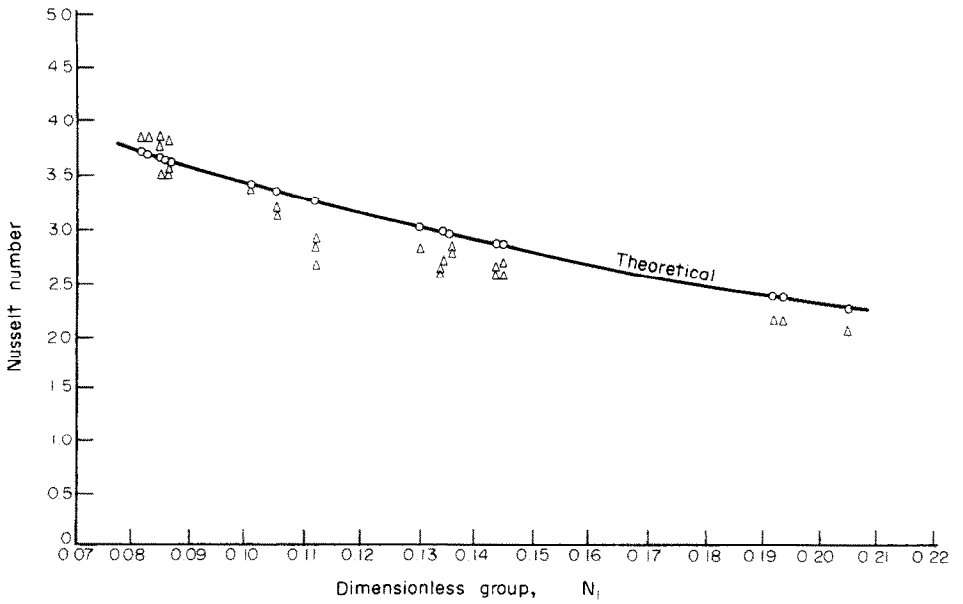

FIG. 6. Plot of Nusselt number against dimensionless group N_1, for single-phase flow. Points are experimental, curve theoretical.

nitrogen at 10 psig through the column at 175°C. The nitrogen was vented after passing through a trap. The column could then be used again.

COMPARISON OF EXPERIMENTAL RESULTS WITH THEORY FOR SINGLE PHASE FLOW

The experimental value of the gas phase heat transfer coefficient was calculated from experimental measurements by use of the equation

$$h_g = \frac{W_g C_g (T_g - T_{gi})}{\pi d L[(T_w - T_{gi}) + (T_w - T_g)]/2} \qquad (23)$$

so that the experimental value of the Nusselt group could be calculated as $h_g d/k_g$.

The theoretical value of the Nusselt group was calculated from equation (10). The physical properties of the gas were estimated at the arithmetic average of gas inlet and outlet temperatures as it was found that the value of the group was insensitive to small changes in gas temperature.

The comparison between experiment and theory is shown in Fig. 6, in which the Nusselt group is plotted against the group $n_1 = \pi k_g L/(4W_g C_g)$ with individual experimental points shown, and the theoretical equation shown as a full line.

Agreement between experiment and theory is close, generally within 10%, although most of the experimental points lie below the theoretical line. The use of an arithmetic average temperature difference, although more satisfactory than logarithmic mean temperature differences, is not strictly correct because of the change of heat transfer coefficient along the tube. A procedure that is free from the use of assumed average temperature differences is simply to compare the temperature rise measured in experiment, with the rise calculated from equation (8). The comparison is shown in Fig. 7, where the much closer agreement is very good evidence of the quality of the model for single phase flow.

Since the mechanism of heat transfer to the gas phase is the same in both the single-phase analysis of Graetz and the two-phase model considered here, Fig. 7 verifies a fundamental part of the model for two-phase flow.

COMPARISON OF EXPERIMENTAL RESULTS WITH THEORY FOR TWO-PHASE FLOW

Visual inspection of the end of the tube showed liquid leaving the serrations in a uniform manner so that there was no experimental evidence of dry spots in the tube. The rate of liquid flow was above the value of minimum wetting rate as estimated from the correlation of Norman and McIntyre [1], and a value of $\psi = 1$ in the experimental model gave the best agreement between theory and experiment when ψ was varied in the computer program. For these reasons the tube was taken to be fully wetted, and ψ was set to 1 in the computation of the model.

The physical properties of liquid and gas used explicitly in the model, i.e. density, viscosity and thermal conductivity of the phases, showed some variations along the tube because of the change in temperature. However, some numerical calculations incorporating these variations gave predicted temperature distributions which differed by less than normal experimental variation from calculations using the physical properties evaluated at the arithmetic average of the appropriate phase temperatures along the tube. The arithmetic average procedure was therefore used in all numerical calculations.

Geraniol was the heat sensitive liquid chosen for the experimental programme because it is desirable that any phase separations involving geraniol and its isomer nerol should be carried out at temperatures no greater than 130–150°C, much lower than the boiling point at 229°C. In consequence the maximum steam temperature was set at 130°C so that no significant thermal degradation took place.

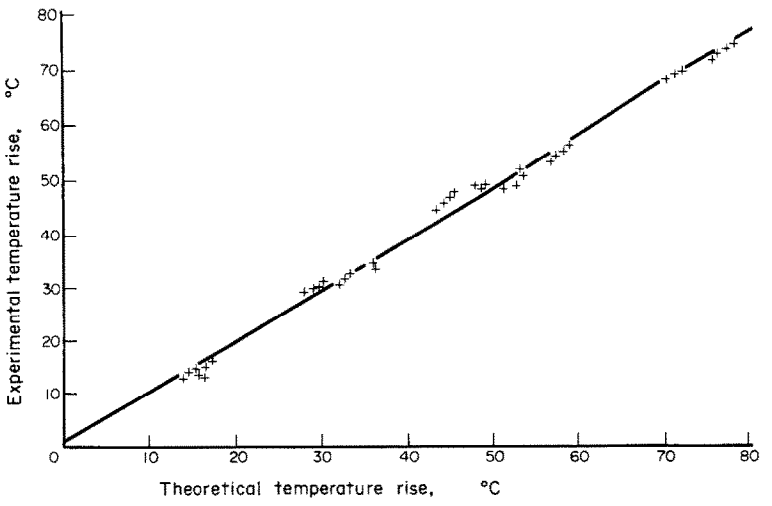

FIG. 7. Experimental vs theoretical temperature rise in gas for single-phase flow.

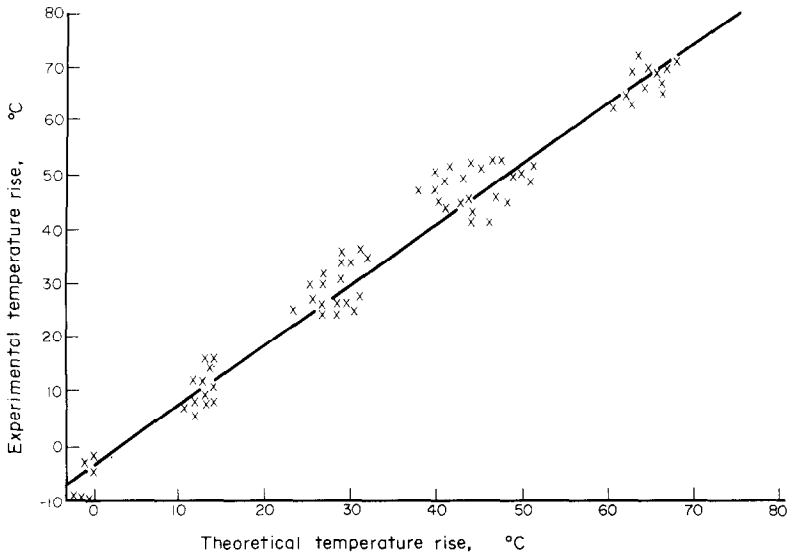

FIG. 8. Experimental vs theoretical temperature rise in gas for two-phase flow.

The vapour pressure of the geraniol was calculated from the interface temperature for each space increment by use of the equation

$$P^*/\text{atm.} = \exp\left(9.2 + \frac{4.97 \times 10^3}{T_a} - \frac{3.82 \times 10^6}{T_a^2} + \frac{3.39 \times 10^8}{T_a^3}\right)\Big/760 \quad (24)$$

an equation that can be fitted to the available vapour pressure data.

Although an effective heat transfer coefficient for two-phase flow could have been calculated, a more direct assessment of the quality of the model, as the comparison for single-phase heat transfer shows, is given by a comparison of gas-phase temperature rise measured in experiment with that found from theory. This comparison is shown in Fig. 8.

The calculated gas temperature was the one parameter which was extremely sensitive to the estimate of the interface temperature used in the model. In helping to establish the validity of the model Fig. 8 particularly demonstrates that the method of estimation was satisfactory.

The five groups of points correspond to different values of the gas inlet temperature which was varied in 20°C stages. A straight line provides an excellent fit to the data whose scatter about the line is independent of temperature rise. The slope of the best fit line, at 1.12, deviates further from unity than in single phase flow (Fig. 6), as might be expected with the greater number of model assumptions and greater scope for experimental variation in the two-phase case. However for the single-phase case agreement between experimental and theoretical temperatures was substantially complete without any indication that the experimental

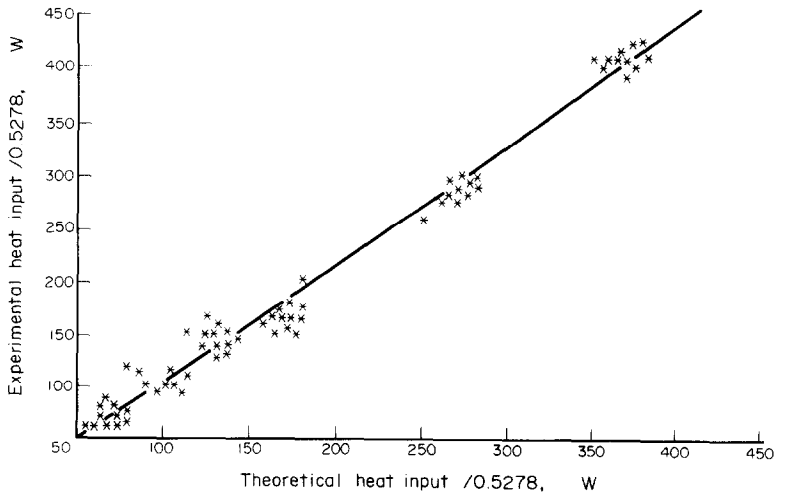

FIG. 9. Experimental vs theoretical heat inputs for two-phase flow.

temperature rise was greater than theoretical.

Another check on the quality of the model was obtained by comparing the experimental and predicted heat inputs. The experimental heat input was the heat given up by the steam condensate less atmospheric losses. The losses were obtained from the corresponding blank (single phase) runs under the same conditions by subtracting the heat gain by the flowing gas from the heat loss by the condensate. The predicted heat input was calculated from the gas and liquid temperature rise and the heat needed for vaporisation. The two heats are plotted against each other in Fig. 9. The slope of the best fitting line is 1.11, in very close agreement with the best fitted line for the gas temperatures. Gas temperatures for two-phase heating are about 10% higher than calculated for theory, but in substantial agreement with theory for single-phase heating.

One possible reason for the difference between experiment and theory might be the validity of the Graetz equations when applied to two-phase flow, in particular the boundary condition of fixed temperature and vapour pressure. However for the experiments the thermal capacity of the flowing liquid was small enough for the liquid surface temperature to approach a steady value close to the tube temperature quite rapidly. In most cases the interface temperature was substantially constant for 90% of the tube length, and this finding, together with the results for single-phase heating, suggests that the Graetz equation is not the source of the difference.

The two independent methods of estimating the interface temperature gave almost identical temperature and pressure profiles and therefore the differences between experiment and theory shown in Figs. 8 and 9 are not thought to be due to the method of estimation.

There is some lack of reproducibility evident in the scatter of the data and similar errors may have occurred because of variations in steam quality, the difficulty in measuring a mean gas temperature with a single thermocouple, or the assumed correspondence between heat losses to the atmosphere in single and two-phase flow.

There is, however, one possible small systematic error that would be evident in two-phase flow but not in single phase flow. Figure 4 shows that the thermocouple measuring the exit gas temperature was placed at the exit of the heated section, but that liquid entered the tube some 3–4 in. above the thermocouple. This length was then available for heat exchange between gas and liquid so that the liquid temperature when it reached the thermocouple level was greater than the temperature of the liquid pool before entering. Since liquid temperatures on entering were mainly below the gas temperature on leaving, the effect of this additional length is to give a higher gas temperature at the thermocouple than would be predicted by the model. The experimental configuration at that point would preclude an accurate estimate of this correction, but the order of magnitude and sign of the correction are similar to differences shown in Fig. 8, and we conclude that this experimental feature is the most likely reason for the differences.

Bearing in mind this small error and other minor uncertainties we may regard the agreement between model and experiment as very satisfactory.

EFFECT OF OPERATING CONDITIONS ON EVAPORATOR PERFORMANCE

The effect of liquid and gas flow rates and inlet temperatures on the performance of the evaporator may be deduced from the temperature and vapour pressure profiles in the tube predicted by the model. Profiles were computed for a variety of combinations of flow rate and inlet conditions corresponding to some of the operating parameters used in the experimental study. Gas flow rates ranged from 10 to 25 dm^3

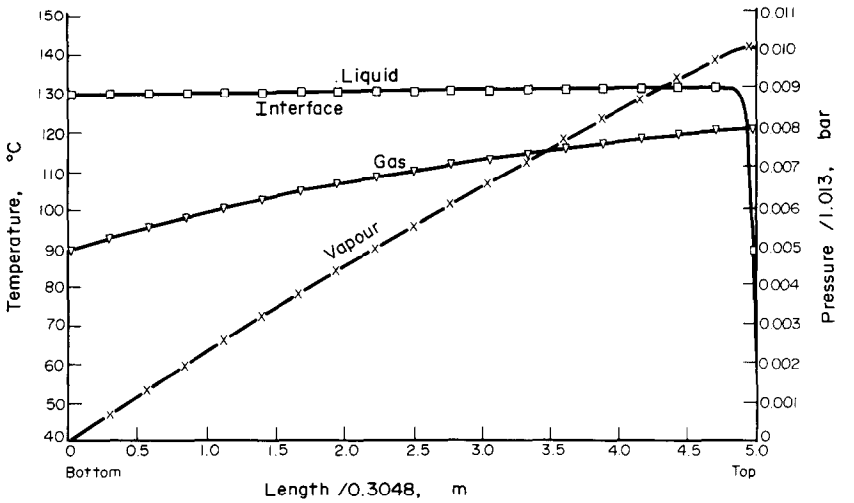

FIG. 10. Temperature and pressure profiles for conditions: $T_{gi} = 39.6°C$, $T_{gi} = 90°C$, liquid flow = 30 cm^3 min^{-1}, gas flow = 20.9 × 10^3 cm^3 min^{-1}. Interface and liquid temperatures are identical.

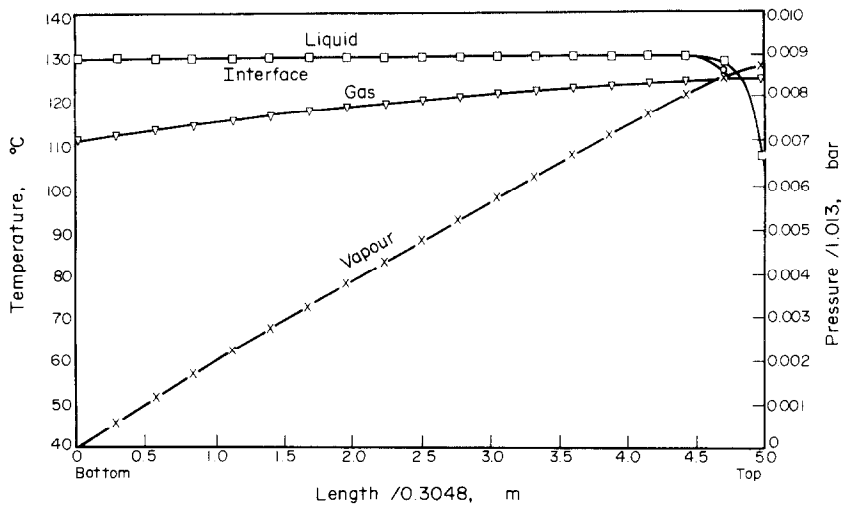

FIG. 11. Temperature and pressure profiles for conditions: T_{li} = 100.7°C, T_{gi} = 111.3°C, liquid flow = 70 cm^3 min^{-1}, gas flow = 26.8 × 10^3 cm^3 min^{-1}. Interface temperatures are identical to liquid temperatures except where shown by ○.

min^{-1}, gas inlet temperatures from 50 to 130°C, liquid flow rates from 30 to 70 cm^3 min^{-1} and liquid inlet temperatures from 40 to 100°C. Three of these profiles, illustrating different conditions, are shown here in Figs. 10–12. The main conclusions drawn from these and other profiles, and confirmed, where appropriate, by experimental data, are as follows.

The flow rate and inlet temperature of the gas have little effect on the liquid temperature profile, provided that flooding (liquid flow reversal) is avoided. (Flooding occurred only at gas flow rates over 28 dm^3 min^{-1} in conjunction with liquid flow rates of about 70 cm^3 min^{-1}). Under all conditions studied the liquid exit temperature is within 1°C of the wall temperature. Gas flow rate is the major factor determining the vapour pressure of the diffusing component achieved at the gas exit. Under the conditions of Fig. 10 a rise in gas flow from 20.9 to 26.9 dm^3 min^{-1} produces a 13% fall in vapour pressure. The only significant effect of a 40°C reduction in gas inlet temperature from 110°C is to decrease the gas outlet temperature by about 13°C under the conditions of Fig. 11. Raising the liquid flow rate from 30 to 70 cm^3 min^{-1} greatly increases the thermal entrance length for liquid (about four times in Fig. 12) and reduces the vapour pressure by a few per cent but has little effect otherwise. Most surprising, perhaps, is the lack of influence of the inlet temperature of the liquid on performance. As illustrated in a comparison of Figs. 11 and 12, the liquid entrance length increases by about 70% as the liquid inlet temperature goes from 40 to 100°C (wall temperature constant 130°C), but there is little change in any exit condition. This behaviour reflects the poor heat transfer characteristics of the gas as compared with the

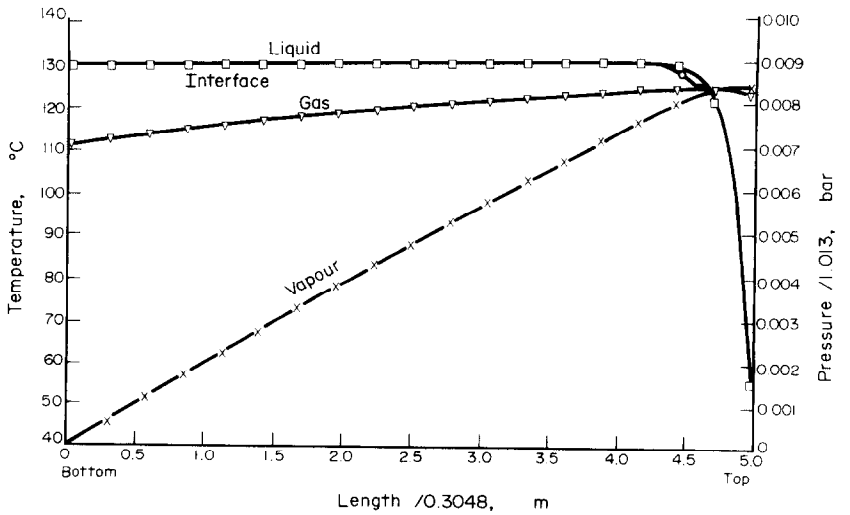

FIG. 12. Temperature and pressure profiles for conditions: T_{li} = 39.3°C, T_{gi} = 111.3°C, liquid flow = 70 cm^3 min^{-1}, gas flow = 26.8 × 10^3 cm min^{-1}. Interface temperatures are identical to liquid temperatures except where shown by ○.

liquid film, and associated short thermal entrance length for liquid. Partly for the same reason the region of cold liquid at the top of the tube causes negligible condensation of vapour. The largest fall in vapour pressure observed, about $\frac{1}{2}\%$, occurs only under the most extreme combination of conditions studied, viz. with a liquid feed at the highest flow rate (70 cm^3 min^{-1}) and lowest temperature (40°C) (Fig. 12).

ASSESSMENT OF EVAPORATOR PERFORMANCE

The computed rate of vaporisation varies from a minimum of 0.50 to a maximum of 0.84 cm^3 min^{-1}. The maximum rate is achieved with the highest gas flow rate (25 dm^3 min^{-1}), highest gas inlet temperature (130°C) and highest liquid inlet temperature studied (100°C) and the lowest liquid flow rate (30 cm^3 min^{-1}). The highest vapour pressure, however, is attained with the lowest gas flow rate of 10 dm^3 min^{-1}. The vapour pressure is then 0.015 bar, corresponding to a mole fraction of 0.0085. The gas at exit is only 47% saturated, a fact reflected in the near-linearity of the vapour pressure profile and the negligible condensation of vapour in contact with cool liquid at the top of the tube. The low rate of evaporation is a consequence of low saturation vapour pressure and low rates of gaseous diffusion at the temperatures to which the evaporator is restricted by the thermal lability of the diffusing component (130–150°C for geraniol). To give a close approach to the saturation vapour pressure of 0.032 bar at 130°C with geraniol, the tube needs to be about 4 m long. The tube length could be reduced by employing several gas stream passes.

REFERENCES

1. J. G. Collier, *Convective Boiling and Condensation.* McGraw-Hill, New York (1972).
2. J. R. Conder, Performance optimization for production gas chromatography, *Chromatographia* **8,** 60 (1975).
3. L. Graetz, *Ann. Physik* **25,** 337 (1885).
4. W. H. McAdams, *Heat Transmission* p. 230. McGraw-Hill, New York (1954).
5. D. J. Gunn, Transfer of heat or mass to particles in fixed and fluidised beds, *Int. J. Heat Mass Transfer* **21,** 467 (1978).

UN MODELE MATHEMATIQUE POUR L'ECOULEMENT EN FILM LAMINAIRE ET SA VALIDATION EXPERIMENTALE

Résumé—On présente un modèle mathématique pour la vaporisation d'un liquide en écoulement laminaire de film tombant le long de la surface interne d'un tube lisse à contre-courant d'un écoulement laminaire de gaz. Les équations aux dérivées partielles qui décrivent les distributions de température et de composition sont intégrées dans le tube pour donner un système de quatre équations différentielles ordinaires. Une méthode numérique pour la résolution des équations est proposée et examinée; la méthode est posée pour obtenir la réponse transitoire du transfert de chaleur et de masse. Une solution satisfaisante est obtenue pour un domaine spatial et temporel. Le modèle mathématique est validé par des mesures expérimentales sur un évaporateur à film tombant avec des évaporations à des températures inférieures à la température d'ébullition. La qualité de l'évaporateur est déterminée.

WÄRME- UND STOFFÜBERGANG BEI ZWEIPHASENSTRÖMUNG EIN MATHEMATISCHES MODELL DER LAMINAREN FILMSTRÖMUNG UND SEINE EXPERIMENTELLE BESTÄTIGUNG

Zusammenfassung—Ein mathematisches Modell für die Verdampfung von Flüssigkeit aus einem laminaren Film wird beschrieben. Der Film fließt an der inneren Oberfläche eines glatten Rohres im Gegenstrom zu einer laminaren Gasströmung herab. Die partiellen Differential-Gleichungen, die Verteilung von Temperatur und Zusammensetzung beschreiben, werden über den Rohrquerschnitt integriert und ergeben einen Satz von vier gekoppelten gewöhnlichen Differential-Gleichungen. Ein numerisches Verfahren zur Lösung der Gleichungen wird vorgeschlagen und überprüft; diese Methode wird zur Berechnung des instationären Wärme- und Stoffübergangs angewandt. Für einen gewissen Bereich von Raum- und Zeit-Intervallen ergibt sich eine befriedigende Lösung. Das mathematische Modell konnte mit experimentellen Messungen an einem Fall-Film-Verdampfer bestätigt werden, wobei die Verdampfung bei Temperaturen unterhalb des Siedepunktes aus einem laminaren Flüssigkeitsfilm in einen laminaren Gasstrom stattfand. Die Leistung des Verdampfers wird abgeschätzt.

ТЕПЛО- И МАССОПЕРЕНОС ПРИ ДВУХФАЗНОМ ТЕЧЕНИИ. МАТЕМАТИЧЕСКАЯ МОДЕЛЬ ЛАМИНАРНОГО ПЛЕНОЧНОГО ТЕЧЕНИЯ И ЕЕ ЭКСПЕРИМЕНТАЛЬНАЯ ПРОВЕРКА

Аннотация — Представлена математическая модель испарения ламинарной пленки жидкости, стекающей по внутренней поверхности гладкой трубы навстречу ламинарному потоку газа. Дифференциальные уравнения в частных производных, описывающие распределения температуры и состава среды, осредняются по сечению трубы для получения системы из четырех взаимосвязанных обыкновенных дифференциальных уравнений. Предложен и рассмотрен численный метод решения уравнений; высказано предложение, что с его помощью можно получить решение для нестационарных процессов тепло- и массопереноса. Получено удовлетворительное решение для целого ряда пространственных и временных областей. Справедливость математической модели подтверждена результатами опытов на установке со стекающей пленкой, где жидкость при температуре ниже точки кипения испарялась в ламинарный поток газа. Дана оценка производительности такой испарительной установки.